



# University of HUDDERSFIELD

## University of Huddersfield Repository

Kubiak, Krzysztof, Wilson, M.C.T., Mathia, T.G. and Carval, Ph.

Wettability versus roughness of engineering surfaces

### Original Citation

Kubiak, Krzysztof, Wilson, M.C.T., Mathia, T.G. and Carval, Ph. (2011) Wettability versus roughness of engineering surfaces. *Wear*, 271 (3-4). 523 - 528. ISSN 0043-1648

This version is available at <http://eprints.hud.ac.uk/id/eprint/21594/>

The University Repository is a digital collection of the research output of the University, available on Open Access. Copyright and Moral Rights for the items on this site are retained by the individual author and/or other copyright owners. Users may access full items free of charge; copies of full text items generally can be reproduced, displayed or performed and given to third parties in any format or medium for personal research or study, educational or not-for-profit purposes without prior permission or charge, provided:

- The authors, title and full bibliographic details is credited in any copy;
- A hyperlink and/or URL is included for the original metadata page; and
- The content is not changed in any way.

For more information, including our policy and submission procedure, please contact the Repository Team at: [E.mailbox@hud.ac.uk](mailto:E.mailbox@hud.ac.uk).

<http://eprints.hud.ac.uk/>

# Wettability versus roughness of engineering surfaces

K.J. Kubiak<sup>1\*</sup>, M.C.T. Wilson<sup>1</sup>, T.G. Mathia<sup>2</sup>, Ph. Carval<sup>3</sup>

<sup>1</sup> University of Leeds, School of Mechanical Engineering, Institute of Engineering Thermofluids, Surfaces and Interfaces (iETSI), Woodhouse Lane, Leeds LS2 9JT, United Kingdom

<sup>2</sup> Ecole Centrale de Lyon, Laboratoire de Tribologie et Dynamique des Systèmes (LTDS), CNRS UMR 5513, 36 Avenue Guy de Collongue, 69134 Ecully, France

<sup>3</sup> ALTIMET SAS 1, bis Av. des Tilleuls, 74200 Thonon-le bains, France

Corresponding author: [krzysztof@kubiak.co.uk](mailto:krzysztof@kubiak.co.uk), Tel. +44(0)113 343 2107, Fax. +44(0)113 242 4611

[krzysztof@kubiak.co.uk](mailto:krzysztof@kubiak.co.uk)

## Abstract

Wetting of real engineering surfaces occurs in many industrial applications (liquid coating, lubrication, printing, painting...). Forced and natural wetting can be beneficial in many cases, providing lubrication and therefore reducing friction and wear. However the wettability of surfaces can be strongly affected by surface roughness. This influence can be very significant for static and dynamic wetting [1]. In this paper authors experimentally investigate the roughness influence on contact angle measurements and propose a simple model combining Wenzel and Cassie-Baxter theories with simple 2D roughness profile analysis. The modelling approach is applied to real homogeneous anisotropic surfaces, manufactured on a wide range of engineering materials including aluminium alloy, iron alloy, copper, ceramic, plastic (poly-methylmethacrylate: PMMA) and titanium alloy.

**Keywords:** wetting, surface roughness, contact angle, functional surfaces, lubrication.

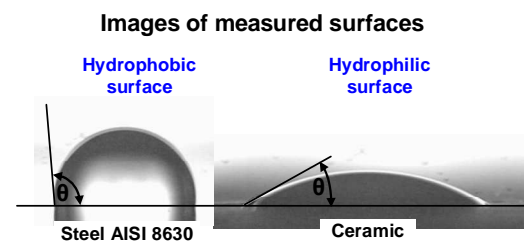
## 1 Introduction

The first recognition of wetting phenomenon in scientific research was given by Galileo in 1612, however it is Thomas Young (1805) who is considered as the father of scientific research on contact angles and wetting [2]. Nowadays many industrial applications like lubrication, painting, liquid coating, spray quenching, soldering, jet-printing etc. involve wetting and spreading processes [3]. These applications often employ high-technology materials and surface preparation to control properties related to wettability: adhesion, anticorrosion, lubrication, friction, wear resistance, biocompatibility, catalysis, antifouling etc. [4, 5, 6].

Though there are many scientific works on molecularly smooth or modelled "simply rough" surfaces [3, 7, 14], little work has been done on wettability and spreading phenomena of real engineering surfaces [8]. By controlling surface roughness different friction properties can be achieved. For smooth but not polished surfaces, reduction in friction and wear is usually observed [9].

Wettability is usually quantified in terms of observed contact angles, so from a practical point of view, a simple methodology is needed to account for the heterogeneous rough surface influence on wetting and contact angle measurements. The first attempt at this was made by Wenzel [10]. His theory was based on the assumption that a rough surface extends the solid-liquid interface area in comparison to the projected smooth surface. This simple model has been found to be useful in capturing experimentally observed influence on the contact angle for simple roughness topography and for well wetting surface where the practical range of the contact angle,  $\theta$ , is

$0^\circ < \theta < 90^\circ$ . The more complex case is that where the contact angle lies in the range  $90^\circ < \theta < 180^\circ$ . In this case, liquid does not penetrate well the rough surface asperities, and gas molecules can be trapped in the asperity valleys. As a result, the interface between liquid and solid is not continuous and there is an alternation of solid-liquid and gas-liquid interfaces. Cassie and Baxter have investigated the wetting phenomenon of composite materials [11], and their theory applied to rough surfaces is able to capture the behaviour of trapped air in the roughness asperities.



| Material properties |                           |         |
|---------------------|---------------------------|---------|
| Metallic            |                           | Ceramic |
| high                | contact angle             | low     |
| poor                | adhesiveness              | good    |
| poor                | wettability               | good    |
| low                 | solid surface free energy | high    |

Figure 1: Examples of measured contact angles and comparison of surface material properties.

To describe the behaviour of real manufactured rough and usually complex surfaces, the combination of these two

theories and surface roughness analysis can give an accurate and comprehensive but still simple methodology. The aim of this paper is to demonstrate such a methodology on real homogeneous anisotropic surfaces, manufactured on a wide range of engineering materials like aluminium alloy, steel, copper, ceramic, poly-methylmethacrylate (PMMA) and titanium alloy (Figure 1).

## 2 Modelling of roughness influence on wettability

Wettability can be defined as the propensity of liquid to spread on a solid surface. The liquid deposited on the solid surface, under gravity has tendency to spread until the cohesion (internal forces) of the liquid, the gravity forces and the capillary (surface tension) forces are in balance, and an equilibrium state is reached. Once equilibrium is achieved, a contact angle,  $\theta_A$ , between the solid surface and liquid can be measured. The equilibrium corresponds to the minimal energy state between the three phases. This state can be described by well-known Young relation [12]:

$$\gamma_{SG} = \gamma_{SL} + \gamma_{LG} \cdot \cos \theta \quad (1)$$

where  $\gamma$  are the surface tension coefficients of solid-gas (SG), solid-liquid (SL) and liquid-gas (LG) interfaces. This theoretical relation is true only for ideally smooth and homogeneous solid surfaces. For rough surfaces, the observed contact angle does not in general match the value seen on ideal surfaces. Below a methodology is described for predicting the observed contact angle on a rough surface from a 2D roughness profile analysis. The model involves combining the well-known Wenzel and Cassie-Baxter theories to capture the influence of surface roughness in the vicinity of the contact line. A 2D roughness profile is appropriate to capture the variation of surface topography along the contact line.

### 2.1 Roughness influence: theoretical and experimental approaches

As mentioned in the introduction, for simply rough surfaces Wenzel's theory can be used [10]:

$$\cos(\theta_A) = r \cdot \cos(\theta) \quad (2)$$

where  $\theta_A$  is an apparent contact angle and  $r$  is the ratio of the real rough surface area to the projected perfectly smooth surface, in other words  $r$  is proportional to the extension of surface area due to the roughness. Note that  $r > 1$  for rough surface and for perfectly smooth surface  $r = 1$  and therefore  $\cos(\theta_A) = \cos(\theta)$ , where  $\theta$  is the contact angle corresponding to the ideal surface [13]. In practice this theory is used for the contact angle range  $0^\circ < \theta < 90^\circ$ . Another attempt to describe the surface heterogeneity has been made by Cassie and Baxter [11]. In the general case, the Cassie-Baxter theory describes the apparent contact angle for a composite material, which is given by the equation:

$$\cos(\theta_A) = \phi_1 \cdot \cos(\theta_1) + \phi_2 \cdot \cos(\theta_2) \quad (3)$$

where  $\phi_1$  is the fraction of interface length and  $\theta_1$  is the contact angle for the first component and  $\phi_2, \theta_2$  the

respective values for the second component. In practice this theory is used in the range of contact angle  $90^\circ < \theta < 180^\circ$ . In a special case where liquid on the heterogeneous rough solid surface leaves gas pockets (where  $\theta_2 = 180^\circ$ ), the Cassie-Baxter equation can be reduced to:

$$\cos(\theta_A) = \phi_{LS} \cdot [\cos(\theta) + 1] - 1 \quad (4)$$

where  $\phi_{LS}$  is the fraction of the liquid-solid interface (hence  $1 - \phi_{LS}$  is the fraction of the liquid-air interface).

For practical applications to real heterogeneous and complex rough surfaces, these two models can be combined together with the application of morphology analysis:

$$\cos(\theta_A) = r \cdot \phi_{LS} \cdot [\cos(\theta) + 1] - 1 \quad (5)$$

In 2D roughness profile analysis the ratio  $r$  can be calculated from the  $R_{Lo}$  (%) parameter and  $\phi_{LS}$  can be obtained from  $R_{mr}$  (%) parameters defined in standard ISO 4287. Here,  $R_{Lo}$  is the developed length of the roughness profile expressed in % of expansion above 100% from smooth profile, hence:

$$r = 1 + \frac{R_{Lo}}{100\%}, \quad (6)$$

and  $R_{mr}$  is the relative material ratio of the roughness profile measured in the vertical position of 25% of maximum height of filtered roughness profile, above the minimal profile point. Depending on the surface roughness complexity only the lower parts of valleys are considered to be able to create the gas pockets and therefore influence the contact line. Therefore, the fraction of the liquid-solid interface  $\phi_{LS}$  can be expressed as:

$$\phi_{LS} = \frac{R_{mr}}{100\%}, \quad (7)$$

Note that 2D profiles for this analysis have been measured in direction perpendicular to the surface texture and along the contact line at point where contact angle was measured.

Another important property of wetting behaviour which can be influenced by surface roughness is contact angle hysteresis [13] which is the difference between the limiting apparent contact angles measured as the contact line just starts to advance and just starts to recede. Usually the hysteresis is greater for the rough surfaces but it is dominated by chemical interactions and heterogeneities rather than roughness itself [14]. In this study we are more interested in the practical applications of wetting phenomenon (like: lubrication, liquid coating, painting, printing ...) and the experimental analysis of contact angle measurements covers only the advancing contact angle. Further investigation is needed to analyse the surface roughness influence on contact angle hysteresis.

### 3 Experiments

Previous investigation of roughness influence on wettability performed by authors [8] pointed out the importance of topographical parameters in 2D and 3D morphology analysis. Statistical covariance analysis showed that in 2D roughness profile analysis the most important parameters are related to the material ratio ( $R_{mr}$  - Relative Material Ratio of the roughness profile,  $T_{rc}$  - Microgeometric material ratio, and  $P_{mr}$  - Relative Material Ratio of the raw profile). Another parameter is  $K_r = AR/2R$  (Mean Slope of the Roughness Motifs) which is defined as the ratio between mean spacing of the roughness motifs (AR) and mean depth of the roughness motifs (R). From a physical point of view, this parameter relates to the surface roughness complexity and is defined by ISO 12085 standard. However, for application of the Wenzel theory more pertinent will be the use of the  $R_{Lo}$  parameter that is geometrically similar to  $K_r$ . The effect of solid surface roughness on wettability is investigated by measuring the contact angle in the direction parallel to the surface texture, i.e. looking across the grooves of the anisotropic surface (Figure 2).

#### 3.1 Materials

A wide range of common engineering materials were selected, in order to evaluate the influence of material properties on wetting phenomenon. Selection of these materials was based on the different properties like electric conductivity, type of material (metallic alloy, ceramic, polymer), and mechanical properties (ductile, brittle and semi-brittle). This allows the influence of material properties to be analysed. All the selected materials are widely used in the manufacturing industry and easily accessible. Tested materials were:

1. Aluminium alloy AA7064,
2. Titanium alloy Ti-6Al-4V,
3. Steel AISI 8630,
4. Copper alloy UNS C17000,
5. Ceramic made from fluorophlogopite mica in a borosilicate glass matrix, with chemical composition: 46% silicon (SiO<sub>2</sub>), 17% magnesium (MgO), 16% aluminium (Al<sub>2</sub>O<sub>3</sub>), 10% potassium (K<sub>2</sub>O), 7% boron (B<sub>2</sub>O<sub>3</sub>), 4% fluorine (F), (machinable glass ceramic).
6. Poly-methylmethacrylate (PMMA).

#### 3.2 Rough surface manufacturing

Tested surfaces were prepared by the abrasive polishing process. The selected process offers mostly smooth mono-directional morphologically oriented surfaces characterized by very high anisotropy [8, 15]. Materials were cut into small cubes (10mm x 10mm x 10mm), with one side polished on different grit sandpapers (80, 400, 600, 2500) to produce a wide range of surface roughness  $R_a = 0.15 - 7.74 \mu\text{m}$ . Measured values of roughness  $R_a$  are presented in Table 1.

Table 1: Average roughness ( $R_a$ ) of prepared surfaces measured on profile perpendicular to the anisotropic surface textures.

| Materials       | Topographical characteristic of tested surfaces $R_a, \mu\text{m}$ |           |           |           |
|-----------------|--|-----------|-----------|-----------|
|                 | Process 1  | Process 2 | Process 3 | Process 4 |
| Aluminium alloy | 0.22   | 0.27      | 0.53      | 3.48      |
| Titanium alloy  | 0.23   | 0.28      | 0.45      | 1.51      |
| Steel alloy     | 0.15   | 0.19      | 0.34      | 1.52      |
| Copper alloy    | 0.21   | 0.26      | 0.4       | 2.52      |
| Ceramic         | 0.38   | 0.59      | 0.98      | 5.54      |
| PMMA            | 0.33   | 0.44      | 1.08      | 7.74      |

Examples of morphologies of prepared surfaces (Surf 1 - 4) measured by optical interferometric profilometry are presented in Figure 3.

#### 3.3 Contact angle measurements

The contact angle between the liquid and tested materials was measured using a PG-X goniometer with image resolution 640x480 pixels. This fully automated apparatus, with integrated pump, delivers accurate droplets in steps of 0.5  $\mu\text{l}$ , and the built-in camera captures a sequence of images to measure the dynamic wetting or the static contact angle at 'equilibrium'. In experiments as a liquid a distilled water were used, which on tested materials gives contact angles in straightforwardly measurable range to minimise measurement uncertainty. The drop volume was taken within the range where the contact angle did not change with the variation of the volume ( $4 \pm 0.5 \mu\text{l}$ ). The principle of operation and position of camera are presented in Figure 2.

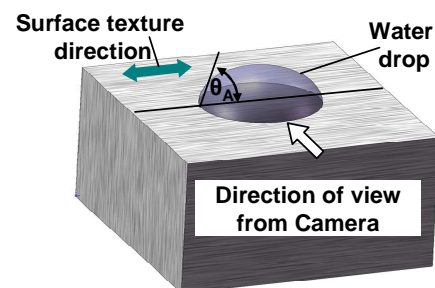


Figure 2: Schematic diagram of experimental measurements of contact angle seen in the direction parallel to surface features.

All specimens were ultrasonically cleaned with alcohol before the test to minimize physical and chemical contamination of the surfaces. Tests were carried out at an ambient laboratory temperature of  $T \sim 22^\circ\text{C}$  and at quasi-constant relative humidity ( $HR \sim 45\%$ ). The equilibrium contact angles were measured after 20 seconds from water drop depositions.

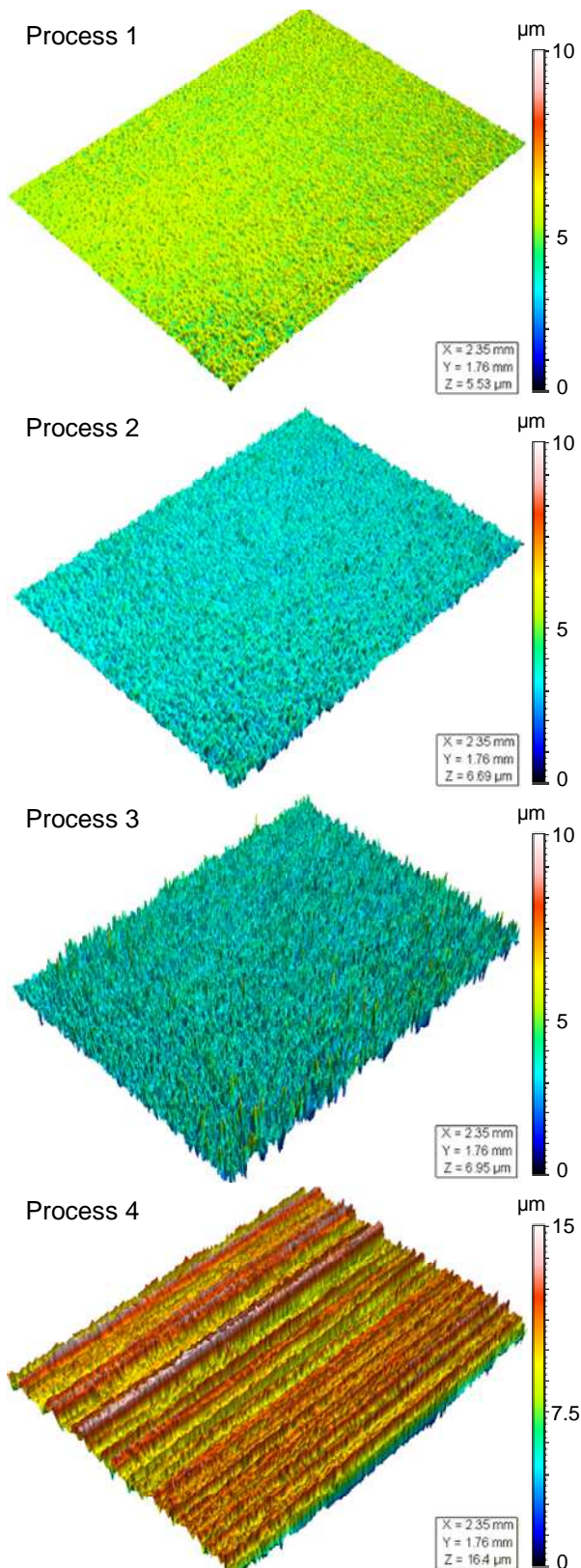


Figure 3: Examples of measured morphologies of tested surfaces prepared by abrasive polishing (material aluminium alloy AA7064) [8].

#### 4 Results

It is recognised that roughness can produce an apparent contact angle, which is different from local one. Due to macroscopic surface roughness, several local equilibrium states on roughness asperities are allowed [16]. Therefore, it is a question of the scale at which one look at the interface.

##### 4.1 Material influence

For all measured surfaces the spreading phenomenon has been observed; after 20 seconds the initial contact angle decreases by 5 to 15 degrees [8].

As a results of the different mechanical properties of tested materials like hardness, plasticity threshold, microstructure, grain size, machinability etc. of each material, slightly different roughnesses were achieved, despite following a similar process preparation procedure for all specimens. This can be seen in the horizontal scatter of corresponding data points between different materials in Figure 4a and 4b. For example, process 4 produced a considerably rougher surface on ceramic and PMMA than it did on titanium or steel alloys.

Figure 4 shows the contact angle measured after 20 seconds for each of the four surfaces prepared on each of the six materials. Low contact angle and good wetting properties can be observed for the ceramic, where the resulting contact angle was 20-40°. Aluminium alloy presents the worst wettability with average contact angle  $\theta_A \sim 83^\circ$ . For steel, titanium and copper materials the average measured contact angles were  $\theta_A \sim 65^\circ$ ,  $\sim 68^\circ$  and  $\sim 65^\circ$  respectively. All these contact angle measurements are consistent with values previously reported in the literature for these and similar materials [17].

Looking now at the effect of roughness, in all cases there is a minimum in the contact angle such that the angle is larger in the small roughness limit, is reduced for intermediate roughness, and then increases with roughness. This is especially noticeable for copper, for which there is a drop of some 30°. Drop of contact angle value in intermediate roughness range is associated with droplet spreading along the grooves [8]. Even small changes in surface roughness can lead to better wetting properties. For example in lubricated contact, such surface texture can act as a reservoir of lubricant.

Figure 5 shows a comparison of a droplet of liquid with the surface asperities, and illustrates that the droplet deposited on the rough surface covers several hundreds of the small peaks and valleys, this present proportion between the roughness and droplet sizes.

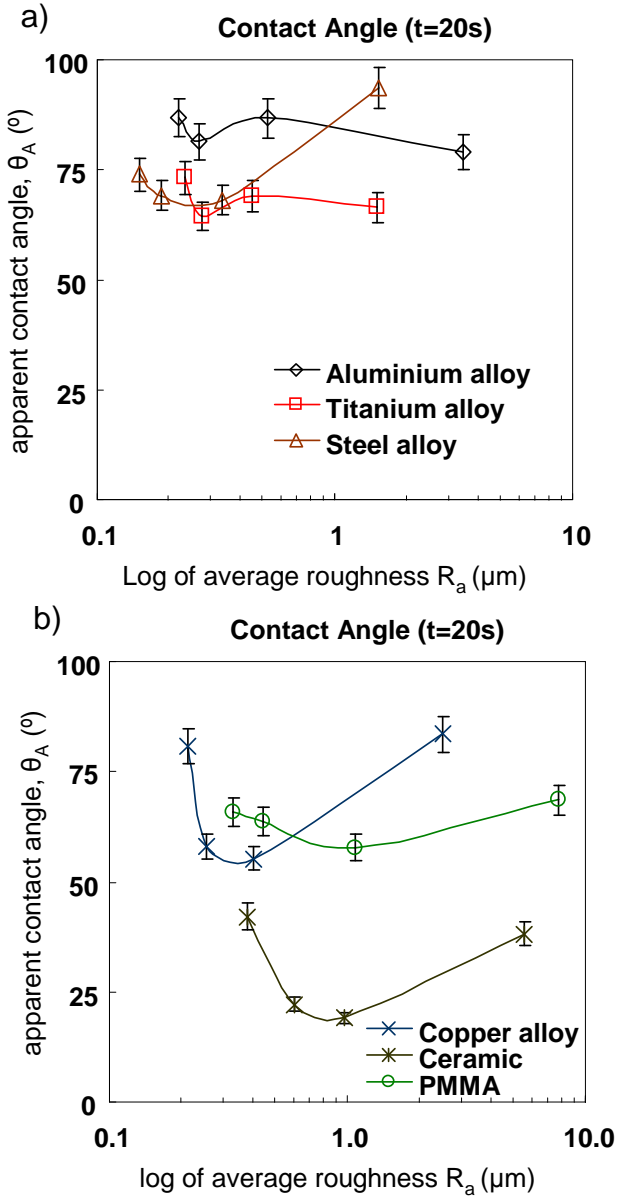


Figure 4: Experimental results of apparent contact angle  $\theta_A$  (t=20s) variation as a function of average roughness parameter  $R_a$ . a) aluminium, titanium and steel alloys, b) copper alloy, ceramic and PMMA materials.

4.2 Roughness analysis, correlation of experimental and modelling

Combining the theories of Wenzel (Eq. 2) and Cassie - Baxter (Eq. 4) with the 2D surface morphology analysis, the apparent contact angle can be modelled by the following equation:

$$\cos(\theta_A) = \left(1 + \frac{R_{Lo}}{100\%}\right) \cdot \left(\frac{R_{mr}}{100\%}\right) \cdot [\cos(\theta) + 1] - 1 \quad (8)$$

where  $\theta$  is the local contact angle (the contact angle on an ideal surface – in practice it can be contact angle measured for a mirror polished surface),  $R_{Lo}$  is the developed length of the roughness profile expressed in % of expansion above 100% from smooth profile and  $R_{mr}$  is relative material ratio of the roughness profile measured in the vertical position of 25% of maximum height of filtered

roughness profile, above the minimal profile point. In this analysis a Gaussian Filter has been used with one cut-off value, where half of the length of a cut-off is amputated from both extremities of a filtered profile. The cut off value was chosen to be 0.08mm in order to analyse roughness and eliminate micro-roughness from profiles. Results of the modelling analysis are summarized in Table 2 and the correlation between the experimentally measured and modelled contact angles for all tested materials is presented in Figure 6.

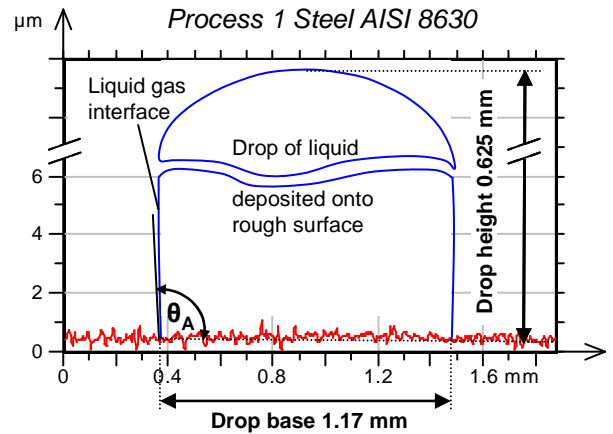


Figure 5: Comparison of roughness profile with size of deposited drop (note that scales on axes are not proportional and drop is deformed) Process 1, material Steel AISI 8630,  $\theta_A=93.7^\circ$ .

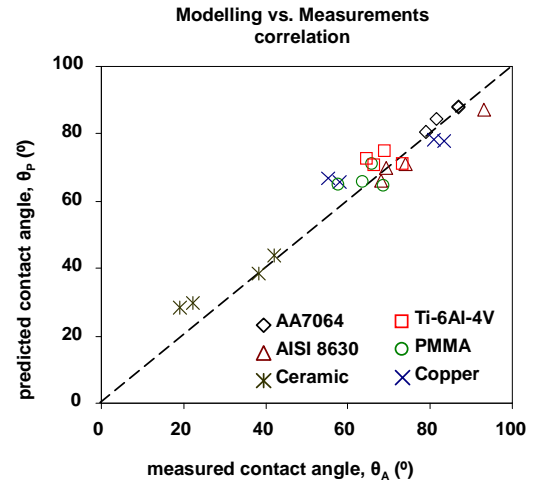


Figure 6: Measured versus modelled contact angle correlation.

Table 2: Contact angle measurements and model predictions based on 2D roughness profile analysis.

| Material (Surface process #) | $R_a$ ( $\mu\text{m}$ ) | $R_{nr}$ (%)<br>(at $0,25 \cdot R_z$ above min filtered profile) | $R_{Lo}$ (%) | Contact angles                 |                    |
|------------------------------|-------------------------|--|--------------|--------------------------------|--------------------|
|                              |                         |  |              | measured $\theta_A$ ( $t=20$ ) | modeled $\theta_P$ |
| AA7064 (Pr.#1)               | 0.22                    | 92.3   | 0.2          | 78.9                           | 88.3               |
| AA7064 (Pr.#2)               | 0.268                   | 98.3   | 0.2          | 86.7                           | 84.5               |
| AA7064 (Pr.#3)               | 0.525                   | 92.6   | 0.6          | 81.4                           | 87.9               |
| AA7064 (Pr.#4)               | 3.48                    | 98.1   | 6.4          | 86.9                           | 80.7               |
| AISI 8630 (Pr.#1)            | 0.15                    | 93.1   | 0.0          | 93.7                           | 71.0               |
| AISI 8630 (Pr.#2)            | 0.186                   | 94.3   | 0.1          | 68.0                           | 69.9               |
| AISI 8630 (Pr.#3)            | 0.338                   | 98.5   | 0.3          | 69.2                           | 66.1               |
| AISI 8630 (Pr.#4)            | 1.52                    | 74.8   | 0.7          | 73.9                           | 85.9               |
| Ceramic (Pr.#1)              | 0.379                   | 92.0   | 0.3          | 38.1                           | 44.1               |
| Ceramic (Pr.#2)              | 0.594                   | 98.9   | 1.4          | 19.1                           | 29.8               |
| Ceramic (Pr.#3)              | 0.975                   | 98.1   | 2.4          | 22.2                           | 29.3               |
| Ceramic (Pr.#4)              | 5.54                    | 87.8   | 9.0          | 42.1                           | 38.5               |
| Copper (Pr.#1)               | 0.212                   | 84.3   | 0.1          | 83.5                           | 78.4               |
| Copper (Pr.#2)               | 0.256                   | 99.0   | 0.5          | 55.3                           | 65.5               |
| Copper (Pr.#3)               | 0.402                   | 96.2   | 0.3          | 57.9                           | 68.1               |
| Copper (Pr.#4)               | 2.52                    | 80.2   | 5.8          | 80.8                           | 78.0               |
| PMMA (Pr.#1)                 | 0.33                    | 90.8   | 0.3          | 68.6                           | 71.1               |
| PMMA (Pr.#2)                 | 0.439                   | 96.6   | 0.5          | 57.8                           | 65.7               |
| PMMA (Pr.#3)                 | 1.08                    | 96.9   | 1.2          | 63.6                           | 64.8               |
| PMMA (Pr.#4)                 | 7.74                    | 87.8   | 12.0         | 65.9                           | 64.5               |
| Ti-6Al-4V (Pr.#1)            | 0.234                   | 96.6   | 0.2          | 66.4                           | 71.0               |
| Ti-6Al-4V (Pr.#2)            | 0.278                   | 94.7   | 0.2          | 69.0                           | 72.5               |
| Ti-6Al-4V (Pr.#3)            | 0.45                    | 92.0   | 0.2          | 64.5                           | 74.7               |
| Ti-6Al-4V (Pr.#4)            | 1.51                    | 95.0   | 2.1          | 73.2                           | 70.8               |

## 5 Discussion and Conclusions

Experimental investigation of the wettability of real surfaces has been performed for a wide range of common engineering materials. Roughness influence on the wetting properties has been evaluated by contact angle measurement analysis. Values of measured apparent contact angle can be strongly affected by the roughness of the measured surface (Figure 4). Therefore, to obtain accurate and reproducible experiment, special attention has to be paid to surface state, and only samples with similar surface roughness should be compared directly. For smooth but not polished surface finishes, where  $R_z$  is in the range 5 to 10  $\mu\text{m}$  (Figure 4), the wettability of the surface is improved. This could be used in many practical applications to adjust surface-liquid interaction. One example could be better lubrication resulting in friction and wear reduction.

To assess the influence of roughness, a simple and practical model of its effect on the apparent contact angle has been proposed. Good correlation between the experimentally measured contact angles and modelled prediction has been found across all the materials considered.

Nevertheless, further investigations are needed to validate this approach for the strongly hydrophobic materials where  $\theta \gg 90^\circ$ . For tested materials, the contribution of Wenzel's model seems to be more important than that of Cassie-Baxter, however these theories combined with simple 2D

roughness profile analysis are complementary and therefore good prediction of the apparent contact angle can be expected for hydrophobic and hydrophilic materials. From the presented investigations the following conclusions can be drawn:

- Roughness has a strong influence on wettability of engineering surfaces,
- Similar influence of roughness has been found for different tested materials,
- The proposed model presents good correlation with experimental data for wide range of tested engineering materials.

## 6 References

- [1] P.G. de Gennes, Wetting: statics and dynamics, *Rev. Mod. Phys.* 57 (3), 827, 1985.
- [2] Robert J. Good, Contact angle, wetting, and adhesion: a critical review, *J. Adh. Sci. Techn.* 6 (12) p1269, 1992.
- [3] K. Narayan Prabhu, Peter Fernades, Girish Kumar, *Materials & Design*, Vol.30, Issue 2, p. 297-305, 2009.
- [4] V. Roucoules, F. Gaillard, T. Mathia, P. Lanteri, Hydrophobic mechanochemical treatment of metallic surfaces. Wettability measurements as means of assessing homogeneity, *Adv. in Colloids and Interf. Sciences*, 97 (1-3), p177-201, 2002.
- [5] Borruto A, Crivellone G, Marani F. Influence of surface wettability on friction and wear tests. *Wear* 222 (1) 57-65, 1998.
- [6] Genzer, Jan and Efimenko, Kirill, Recent developments in superhydrophobic surfaces and their relevance to marine fouling: a review, *Biofouling*, 22: 5, p. 339 - 360, 2006.
- [7] K.M. Hay, M.I. Dragila, J.Liburdy, Theoretical model for the wetting of a rough surface, *J. of Colloid Interf. Science* 325, 472–477, 2008.
- [8] K.J. Kubiak, T.G. Mathia, M.C.T. Wilson "Methodology for metrology of wettability versus roughness of engineering surfaces" *Proceedings of 14<sup>th</sup> Congrès International De Métrologie – Paris, 22<sup>nd</sup> -25<sup>th</sup> June, 2009.*
- [9] K.J. Kubiak, T.G. Mathia, Influence of roughness on contact interface in fretting under dry and boundary lubricated sliding regimes, *Wear*, Vol. 267, p. 315-321, 2009.
- [10] R.N. Wenzel, *Ind. Eng. Chem.* 28, p988, 1936.
- [11] A.B.D. Cassie, S. Baxter, *Trans. Faraday Soc.* 40 p546, 1944.
- [12] T. S. Chow, Wetting of rough surfaces, *J. Physics: Condensed Matter* 10 (27): L445, 1998.
- [13] G. Whyman, E. Bormashenko, T. Stein, The rigorous derivation of Young, Cassie–Baxter and Wenzel equations, *Chem. Ph. Let.* 450, p355, 2008.
- [14] C.W. Extrand, Y. Kumagai, An experimental study of contact angle hysteresis, *J. Colloid & Interf. Science*, 191, 378–383, 1997.
- [15] K J Stout, L. Blunt, W.P. Dong, E. Mainsah, N, Luo, T. Mathia, P. J. Sullivan, H. Zahouani, Development of methods for characterisation of roughness in three dimensions, *Butt.-Heinem.*, ISBN: 1857180232, 2000.
- [16] A. Schwartz, F. Minor, J. Simplified thermodynamic approach to capillarity, *Coll. Sci.* 14, 584, 1959.
- [17] A. Ponter, M. Yekta-Fard, The influence of environment on the drop size - contact angle relationship, *Colloid & Polymer Sci.* 263, p673-681, 1985.